BEAM TRACKING STUDY FOR THE LARGE APERTURE BUMP SYSTEM

M. Shirakata, H. Fujimori and Y. Irie, KEK, Tsukuba, Japan

Abstract

Generally, the magnet aperture tends to be large with respect to the core length for the high intensity accelerators. The effect of the fringe fields on beam may cause the unexpected interferences when the magnet aperture is very large. In joint project of JAERI and KEK, the compact beam bump system is required for the beam injection of the 3 GeV rapid cycling synchrotron (RCS). The eight magnets bump system is under consideration, here. The core length of bump magnets cannot be so long and the strong fringe fields are expected. Because the distance between the adjacent bump magnets is also close, the fringe fields enhance or overlap each other and the magnet effective lengths change dinamically. The beam tracking study is discussed of the large aperture bump system with the overlapping fringe fields from the closely aligned bump magnets.

1 INJECTION BUMP SYSTEM

According to the increase of the beam intensity accelerated in the proton synchrotrons, the size of magnet apertures of acceleratores is required to be wider in order to avoid the space charge difficulties from the intense beam, and the fringe field becomes longer for wide aperture magnets. In this paper, we take the injection bump system of the 3 GeV RCS[1] as a target of the tracking study. The injection bump system of the 3 GeV RCS consists of eight septum-type magnets as shown in Fig.1. The bump magnets are placed each other in close because of the length limitation of the straight section.[1] The physical parameters of magnets are listed in Table 1.

Table 1: Physical parameters of the bump magnets. Positive kick means that the orbit bends toward the x direction.

Magnet	Gap Height [mm]	Physical Core Length [mm]	Kick Angle [mrad]
OB1	184	250	+54.287
OB2	184	250	-47.534
IB1	194	300	+55.852
IB2	194	214	-55.852
IB3	140	255	-76.833
IB4	140	300	+76.833
OB3	134	300	-76.833
OB4	134	300	+70.080

[1]In the present day, the 3 GeV RCS design has been completely changed. The distances between each bump magnet are much longer in the new injection system.

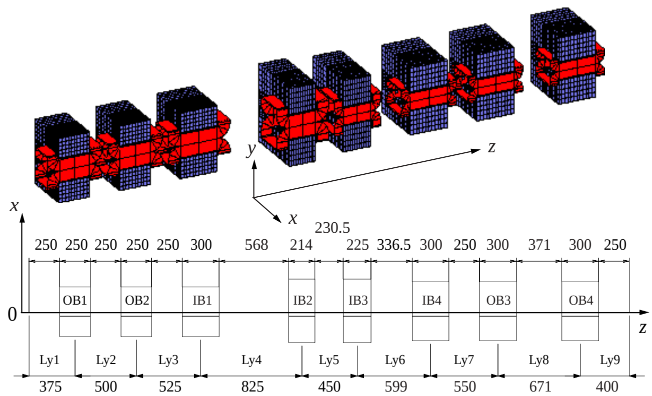

Figure 1: Layout of injection bump system which consists of 8 septum-type magnets.

The magnetic fringe fields are overlapped each other and the perturbation from the neighboring iron cores distorts the field shapes. The resulting magnetic field is not a simple sum of the fields of bump magnets. In this case, it is necessary to treat the whole bump system as a single element with a structured magnetic field.

2 FIELD CALCULATION

The magnetic field of the eight bump magnet system was calculated by the OPERA-3d code, where the permeability is assumed for the case of iron. Since the number of meshes for calculations is limited to less than 150,000, 20 mm at the minimum mesh size in each direction was adopted to cover entire volume of the magnet area as shown in Fig.1. The distribution of B_y along the central trajectory (x = 100 mm) is shown in Fig.2. The excitation current for each magnet has been so adjusted that the field integration in each domain (BL-product) gives a required kick angle in Table 1.

Table 2: BL adjustment

Magnet	BL [T mm]		Ratio [%]	
	(required)	(calculated)	before adj.	after adj.
OB1	172.8	165.0	95.5	99.6
OB2	151.3	134.2	88.7	100.4
IB1	177.8	167.0	93.9	99.8
IB2	177.8	169.9	95.6	100.0
IB3	244.6	233.4	95.4	99.9
IB4	244.6	231.7	94.7	100.0
OB3	244.6	235.5	96.3	100.0
OB4	223.1	221.6	99.3	100.0

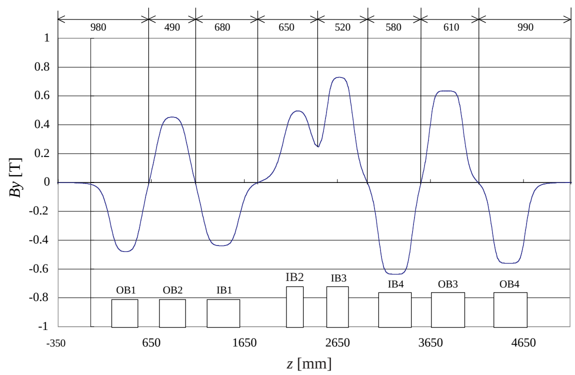

Figure 2: Distribution of B_y along the central trajectory ($x = 100$ mm). Field integration domain for each magnet is shown by vertical bars.

In order to see the field interferences in a closely aligned magnet system, the field distributions were also calculated when the magnet is located separately far from other magnets. Fig.3 shows the comparison of the superimposed result of the solitary excited fields and that of the whole field analysis for the real arrangement around OB2. The peak field of the middle magnet(OB2) is reduced by 1.8%, although the fringing field almost coincides for both cases. Table 2 shows the reduction of the field integration in the real arrangement compared to that of the separate magnet. When the magnets are closely located each other, BL-products must be adjusted from the separate field calculation. The ratio of the field integration after adjustment to the required one is also shown in Table 2. Such field interferences between magnets depends upon the excitation level of the neighboring magnets. Keeping the currents in IB1-4 constant, the currents in outer bumps (OB1-4) were changed down to half and zero. Table 3 shows variations of the field integration, where it is clearly seen that the magnets at both sides are influenced by the current changes. The magnet used in this study is a septum-type magnet. The BL-product variation of OB2 with respect to x-coordinate has a form of

$$B_y = 1 + 6.16 \times 10^{-2}x - 6.19x^2 + 2.03x^3 \qquad (1)$$

where x is defined in meter, when expanded around $x = 100$ mm.

Table 3: Bump balance dependency upon the OB magnets excitation

Magnet	Bump balance ratio [%]		
	OB full	OB 1/2	OB zero
IB1	99.8	101.2	104.4
IB2	100.0	100.0	100.0
IB3	99.9	99.9	99.9
IB4	100.0	100.8	102.6

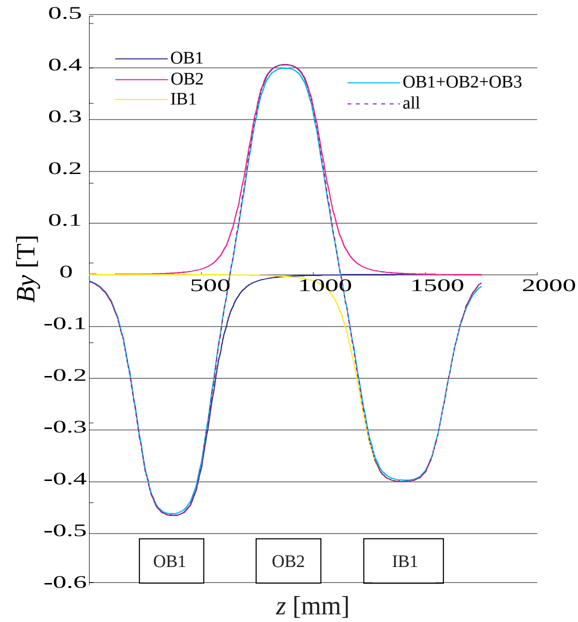

Figure 3: Magnetic field difference between the superimposing and the whole field analysis.

3 PARTICLE TRACKING

The particle tracking is carried out by using TRACY-II particle tracker code which has been developped at the KEK. In order to describe the structured magnetic field, we introduced a ‘meshed element’ into the tracking simulation. The meshed element consists of divided cell blocks as shown in Fig.4. The magnetic field is defined at the center of each cell and represented by the center value.

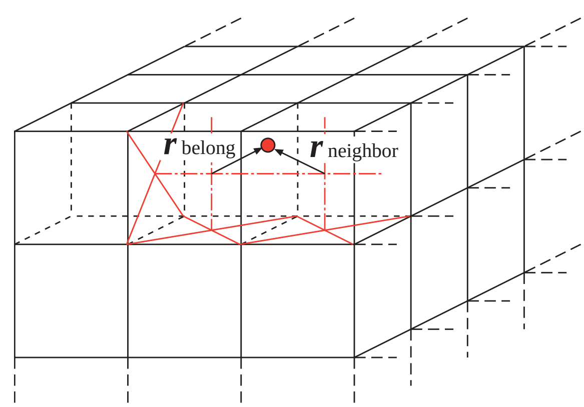

Figure 4: Layout of meshed element.

The particle trajectory is traced by solving the 3D differential equations with the Runge Kutta method in the GenericSolver which was newly developped for the TRACY-II optional subprogram. The GenericSolver is mainly applied to the fringing fields, moreover, it can trace the returning[2] and spiraling particles[2]. The meshed element was defined

[2]The trajectory of the stripped electron from the H^- injection foil was analysed.

in the area of -100 ≤ x ≤ 270, -105 ≤ y ≤ 105 and 0 ≤ z ≤ 4900 mm for the injection bump system. The cell size is 10 × 10 × 10 mm. The magnetic field is only defined at the cell center. The linear approximation is carried out for the magnetic field at the particle position as follows:

$$B = \frac{B_{\mathbf{belong}} r_{\mathbf{neighbor}} + B_{\mathbf{neighbor}} r_{\mathbf{belong}}}{r_{\mathbf{belong}} + r_{\mathbf{neighbor}}} \qquad (2)$$

where B is a magnetic field and r means a distance between the cell center and a particle. The suffix indicates the relation of the cell with respect to a particle. The cell 'belong' means that it contains a particle in it. The cell 'neighbor' means that it is the nearest one among 26 cells which surround the cell 'belong'. If the cell size is small enough with respect to the field structure, the field approximation is not always necessary. The effect from the field approximation onto the tracking results is not so large when the cell size along the beam line was changed to 2 mm from 10 mm. But the field linear approximation method is the default though the difference is small enough in many cases.

Generally, this method does not insure the symplecticity conservation. In order to estimate the unexpected deviation from the calculation errors, we have tested with the ideal meshed element which has a hard-edged field structure. With the ideal meshed element, the tracking result is expected to be the same one of the thin lens approximation in the first order. Because the field's hard edge must be defined at the mesh border, the magnet position and length of IB2 and IB3 is modified about 5 mm. Though this modification brings about the closed orbit distortion of about ± 1.4 mm on the particle trajectory, it is not essential for the code verification. It was found that the tracking deviation was about up to ± 0.2 mm and the anomalous divergence could not be observed for 10000 turns. Because the injection process of the 3 GeV RCS ends before 310 turns, there is no need to worry about the symplecticity violation.

The result of the tracking simulation of the injection bump system by TRACY-II with GenericSolver is shown in Fig.5 and Fig.6. The injection bump system was analysed as a single system which has a complex structured magnetic field given in Fig.2, and the momentum deviation was assumed to be zero $\Delta p/p = 0$, here. The acceptance of the injection bump system is estimated to about 430 π mm mrad. The geometrical acceptance for the center momentum particles is estimated to be 556 π mm mrad. It can be considered that the acceptance decrease comes from the magnet fringe fields and the bump orbit distortion.

4 SUMMARY

- The simulation method has been established with complex magnetic fringe fields.
- The magnetic field must be calculated taking into account the neighboring magnets.
- The acceptance of injection system decreases from 556 to 430 π mm mrad due to the fringe fields and the orbit distortion.

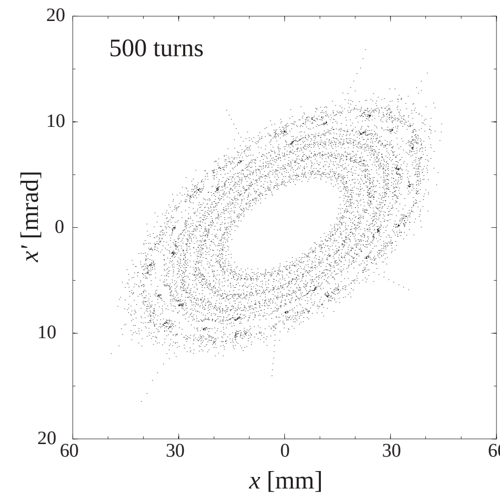

Figure 5: Poincaré map at the entrance of the injection bump system.

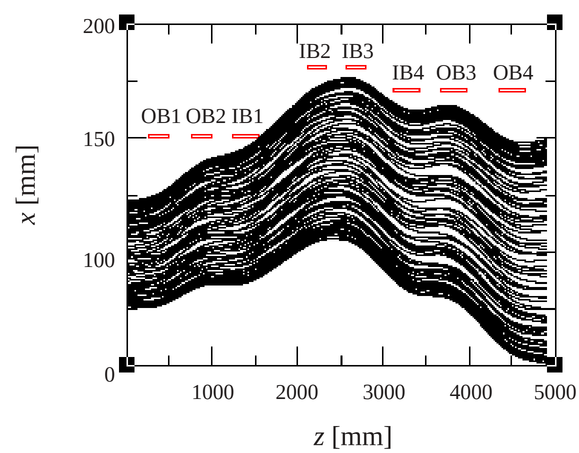

Figure 6: Orbit in the injection bump system. Red boxes indicate the septa for each magnet and the inner side limitation is at $x = 0$ mm.

- The tracking method described in this paper will be applied to the present 3 GeV RCS injection system.

5 REFERENCES

[1] KEK Report 97-16, JHF-97-10, March 1998

[2] I. Sakai et al., ID:1175, THPLE007, EPAC 2002, Paris, June 2002.